Int J Earth Sci (Geol Rundsch) (2017) 106:899–915
DOI 10.1007/s00531-016-1340-1

ORIGINAL PAPER

Subsurface mapping in the Iberian Pyrite Belt using seismic reflection profiling and potential-field data

João Carvalho[1] · Carlos Inverno[1] · João Xavier Matos[1] · Carlos Rosa[1,4] · Isabel Granado[1] · Tim Branch[2] · Patrícia Represas[1] · Livia Carabaneanu[2] · Luís Matias[3] · Pedro Sousa[1]

Received: 9 January 2015 / Accepted: 22 May 2016 / Published online: 15 June 2016

Abstract The Iberian Pyrite Belt (IPB) hosts world-class massive sulphide deposits, such as Neves-Corvo in Portugal and Rio Tinto in Spain. In Portugal, the Palaeozoic Volcanic-Sedimentary Complex (VSC) hosts these ore deposits, extending from the Grândola-Alcácer region to the Spanish border with a NW–SE to WNW–ESE trend. In the study area, between the Neves-Corvo mine region and Alcoutim (close to the Spanish border), the VSC outcrops only in a small horst near Alcoutim. Sparse exploration drill-hole data indicate that the depth to the top of the VSC varies from several 100 m to about 1 km beneath the Mértola Formation Flysch cover. Mapping of the VSC to the SE of Neves-Corvo mine is an important exploration goal and motivated the acquisition of six 2D seismic reflection profiles with a total length of approximately 82 km in order to map the hidden extension of the VSC. The data, providing information deeper than 10 km at some locations, were integrated in a 3D software environment along with potential-field, geological and drill-hole data to form a 3D structural framework model. Seismic data show strong reflections that represent several long Variscan thrust planes that smoothly dip to the NNE. Outcropping and previously unknown Late Variscan near-vertical faults were also mapped. Our data strongly suggest that the structural framework of Neves-Corvo extends south-eastwards to Alcoutim. Furthermore, the VSC top is located at depths that show the existence within the IPB of new areas with good potential to develop exploration projects envisaging the discovery of massive sulphide deposits of the Neves-Corvo type.

Keywords Iberian Pyrite Belt · Massive sulphide deposits · Volcanic-Sedimentary Complex · Seismic reflection · Magnetic anomalies · Bouguer anomalies

✉ João Carvalho
joao.carvalho@lneg.pt

Carlos Inverno
carlos.inverno@lneg.pt

João Xavier Matos
joao.matos@lneg.pt

Carlos Rosa
carlos.rosa@edm.pt

Isabel Granado
isabel.granado@lneg.pt

Tim Branch
tim.branch@prospectiuni.com

Patrícia Represas
patricia.represas@lneg.pt

Livia Carabaneanu
livia.carabaneanu@prospectiuni.com

Luís Matias
lmatias@fc.ul.pt

Pedro Sousa
pedro.sousa@lneg.pt

[1] Laboratório Nacional de Energia e Geologia, Apartado 7586-Alfragide, 2710-966 Amadora, Portugal

[2] Prospectiuni S.A., Strada Caransebeș 1, București, 012271 Bucarest, Romania

[3] Instituto Dom Luiz, Faculdade de Ciências, Universidade de Lisboa, Campo Grande, 1749-016 Lisbon, Portugal

[4] Present Address: Empresa de Desenvolvimento Mineiro (EDM), Rua Sampaio e Pina, 1 – 3.Dto., 1070-248 Lisbon, Portugal

Introduction

The knowledge of the Variscan structure with depth is essential for ore exploration in the Iberian Pyrite Belt (IPB) area. Metallic ore deposits, such as the massive sulphide deposits of the IPB, are often associated with dipping (30°–60°) structures. Strong deformation and metamorphism limit the use of seismic methods to locate them. Reflection seismic methods had long been employed to study the tectonics and stratigraphy of sedimentary basins, where acoustic impedance contrasts are generally strong enough to allow mapping of the subsurface geological features. Recent developments in migration algorithms, signal-to-noise ratio (SNR) enhancement, such as in the common-reflection surface (CRS) method can improve the mapping of such deposits in structurally complex environments (e.g. Mann et al. 1999, 2007; Hubral 1999). 3D seismic profiling and advances in electronics such as 24-bit A/D converters have also contributed to improving the utility of reflection seismic methods in hard-rock environments (e.g. Cordsen et al. 2000; Vermeer 2002; Eaton 2003).

In the last decades, the seismic reflection method has experienced a dramatic increase in the number of applications to hard-rock exploration (e.g. Kim et al. 1994; Radzevicius and Pavlis 1999; Juhlin et al. 2002; Juhlin and Stephens 2006; Eaton 2003; Schmelzbach et al. 2007; Malehmir et al. 2012a; Heinonen et al. 2013; Ehsan et al. 2014). The mining sector is one of the fields where the seismic reflection method has shown great utility to complement the more generally applied gravimetric, magnetic, electrical and electromagnetic methods. When combined with traditional methods, reflection seismic method can provide structural information in complex geological environments (Manzi et al. 2012, 2013).

Both 2D and 3D seismic methods have now provided successful case histories in the mining industry (Adam et al. 1998; Calvert and Li 1999; Ayarza et al. 2000; Cheraghi et al. 2011, 2012; Malehmir et al. 2011, 2012a, b; Urocsevic et al. 2012; Ahmadi et al. 2013). On the Portugal mainland, the first seismic reflection profiles acquired in Alentejo for this purpose were supported by Somincor, the mining company operating in the Neves-Corvo mine, in 1991 and 1996 (Carvalho et al. 1996). Twelve profiles were shot by Compagnie Générale de Géophysique (CGG) using explosives as a seismic source and a system of 48 or 24 active channels. At the time, the results were of poor quality and were not very useful to the local mining companies and no further surveys were acquired during the following years.

Several years after the last CGG survey in Portugal, the first deep seismic reflection profiling started in the Spanish part of the IPB, close to the Portuguese border. For the first time, the whole crust down to Moho was imaged in the area, giving unprecedented information about the rooting of several outcropping structures and geological formations (e.g. Simancas et al. 2003; Carbonell et al. 2004). In Portugal, useful results were obtained using seismic reflection and gravimetric modelling for shallow massive sulphides exploration in the western section of the IPB. Geophysical data were used to define the depth to the Palaeozoic basement beneath the Cenozoic sedimentary cover (Oliveira et al. 1998; Carvalho et al. 2011).

Encouraged by these results, under the scope of the EU Seventh Framework Programme (FP7)-funded Promine project, it was decided to acquire a set of 2D seismic reflection profiles to provide structural information down to 4–5 km in the SE sector of the Portuguese IPB region (Inverno et al. 2015a). The aim was to determine whether the structural framework associated with the Neves-Corvo mine, together with a lineament of Late Variscan vein-type Cu occurrences, extends SE to the Spanish border, south of Alcoutim (Carvalho 1991; Matos et al. 2003; Reiser et al. 2011), as suggested by several holes drilled in the flysch cover represented by the Mértola Formation shales and greywackes of Upper Visean age (Oliveira et al. 2004). These data would also help to outline the upper and lower limits of the Volcanic-Sedimentary Complex (VSC) in the region. The use of seismic profiles could also allow acquisition of information about the IPB basement, which at the Neves-Corvo region is constituted by the Phyllite–Quartzite Group (PQG) of Famennian age (Oliveira et al. 2013). Therefore, in the scope of this work, seismic reflection data were acquired, processed and interpreted together with geological 1/200 000 scale mapping, drill-hole data and information from different surveys: aeroradiometric (gamma-ray total counts), land gravimetric and aeromagnetic data in a 3D modelling environment.

The seismic reflection method is the most suited for the purpose of geological mapping of the IPB due to its superior resolution and depth penetration. Drill-holes usually do not exceed a depth of 2 km. The available gravimetric data have provided very valuable results for the discovery of several important mineral deposits such as Neves-Corvo. However, not only are these data affected by the traditional non-uniqueness problems associated with inversion (e.g. Menke 2012), but also generally do not provide useful information below a depth of 1–2 km. Electrical and electromagnetic methods, often applied in the area, are useful for locating ore bodies down to 1–2 km, but they do not provide detailed structural information, such as the location of major thrust planes and faults.

The knowledge of the Variscan structure with depth is essential for ore exploration in the IPB area. Models of the SPZ were until recently based on geological mapping and drill-hole data (not over 2 km depth). The acquisition of the IBERSEIS (e.g. Simancas et al. 2003) and ALCUDIA (e.g.

Martínez-Poyatos et al. 2012) deep seismic reflection profiles in Spain close to the Portuguese border as a part of the SW Iberia EUROPROBE project have provided for the first time valuable information on the Iberian Variscan basement at depth.

Geological setting

The South Portuguese Zone (SPZ) is the southernmost part of the Iberian massif on the south-western Iberian Peninsula and is one of the best exposed fragments of the Variscan orogeny in Western Europe (e.g. Matte 1986). During Late Devonian–Early Carboniferous time, magmatic activity was intense within the SPZ with occurrence of submarine bimodal volcanism that resulted in the generation of world-class massive sulphide deposits (Carvalho et al. 1999; Sáez et al. 1999). This volcanogenic province is usually designated as the Iberian Pyrite Belt (IPB).

The study area within the IPB is located south of Castro Verde, in southern Alentejo Province, south Portugal. It is adjacent to Neves-Corvo mine and extends to the SE to the Spanish border (Fig. 1). The study area is part of the (Middle) Late Devonian–Early Carboniferous IPB succession. This succession is stratigraphically composed of two main distinct sequences (Boogaard 1967; Schermerhorn 1971; Carvalho et al. 1976): the Upper Famennian–Upper Visean Volcanic-Sedimentary Complex (VSC) and the Lower Givetian–Upper Famennian Phyllite–Quartzite Group (PQG; ages in Pereira et al. 2008; Oliveira et al. 2013; Matos et al. 2014; Fig. 1). The VSC is composed of felsic volcanics, basic volcanics, black shales, siltstones, volcanogenic sedimentary rocks, cherts and jaspers.

The IPB sequence is stratigraphically overlain by marine sedimentary rocks of the Baixo Alentejo Flysch Group (BAFG), represented in the study area by the Mértola Formation (Upper Visean) and by the Mira Formation (Upper Visean–Serpukhovian; Carvalho et al. 1976; Oliveira 1983; Matos et al. 2003; Oliveira et al. 2004; Pereira et al. 2008). A considerable amount of palynological, ammonoid and geochronological ages have been determined on these units. The Mértola Formation at depth was recognized by exploration drill-holes, showing variable thickness, locally >1 km. At Neves-Corvo (see location in Fig. 1) and NW of

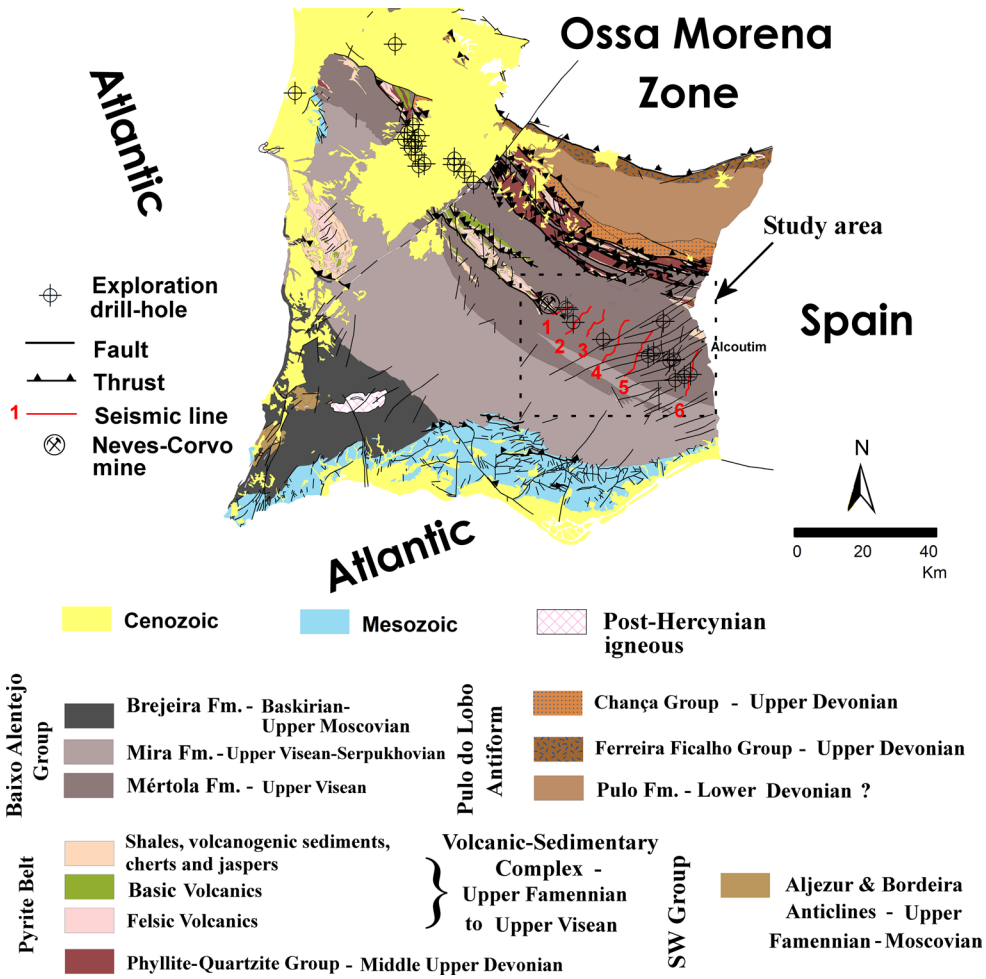

Fig. 1 Geological sketch (after Oliveira et al. 1992) and location of the study area, which is indicated by the *dashed line*

the Alcoutim VSC horst structure, the Mértola Formation is present in duplex tectonic structures dominated by thrusts, located between VSC units. North of the IPB, different metasedimentary units of Lower Devonian–Upper Famennian age crop out, namely the Pulo do Lobo Formation, in between the Chança Group and the Ferreira-Ficalho Group (Fig. 1; Oliveira et al. 2004).

The study area is located between the Neves-Corvo mine (Fig. 1), in the SE sector of the Neves-Corvo–Rosário antiform, and the Spanish border, located 50 km to the south-east (Fig. 1). It comprises four main antiformal structures, Castro Verde-Casével, Neves Corvo-Rosário, Panóias-Ourique, and possibly Alcoutim (see location in Fig. 1). These structures are all placed along distinct volcanic axes. The exposed VSC lithologies are dominant in these antiforms. The PQG is only exposed locally at the SE area of the Rosário antiform (Oliveira et al. 2013) and at depth in the Neves-Corvo mine (Relvas et al. 2006; Pereira et al. 2008).

The geological sequence is represented from base to top by the PQG (>100 m thick), of Upper Famennian to Strunian age, that forms the IPB siliciclastic lower group and consists of shales, siltstones and quartzites, with limestones on top of the succession; and the VSC, which starts with a Famennian lower VSC sequence (500 m thick), with rhyolites, rhyodacites, volcaniclastic sedimentary rocks, shales, basalts and dolerite sills (Oliveira et al. 2013). The Neves-Corvo sulphide ores are associated in this lower VSC sequence with black shales of the Neves Formation, of Strunian age (Pereira et al. 2008), and felsic volcanics and are represented by seven massive sulphide lenses and related stockworks.

In the mine area, the lower VSC is unconformably overlain by the Visean Mértola Fm. (Mt2) greywackes and shales (up to several decametres thick; Pereira et al. 2008; Oliveira et al. 2013). The Upper Visean VSC sequence (≈450 m thick) is present, after a Tournaisian gap, on top of those turbidites. Shales, such as grey to black shales, purple shales, and shales with phosphate nodules, and chert, fine volcanogenic sedimentary rocks and felsic volcanic rocks, are part of this sequence. The upper VSC sequence is overlain by the Visean Mértola Fm. (Mt1; older than Mt2) [>1000 m thick], dominant in the study area, with greywackes, siltstones and shales. In the SW part of the study area, the younger Mira Fm. (1000–2500 m thick) occurs SW of the Mértola Fm., with fine-grained greywackes, shales and siltstones. Within the study area, the VSC outcrops only at the SE area of the Rosário–Neves-Corvo structure and in the Alcoutim horst (Fig. 1; Leca 1976; Leca et al. 1983; Oliveira et al. 2013). A thrust between the upper VSC and Mt2 (flysch) is a distinctive guide in the mine area to the Neves-Corvo ore horizon which is represented by the black shales of the Neves Formation and felsic volcanics (Carvalho 1991).

All these stratigraphic units are affected by Variscan NW-trending folds and associated (main) cleavage dipping 60°–70° to the NE, with vergence towards SW (Oliveira et al. 2004). The Neves-Corvo–Rosário antiform (VSC–PQG) plunges at low angle to the SE under the exposed Mértola Fm. rocks, as indicated by a few drill-holes and different types of geophysical surveys. Several thrust faults parallel to the main cleavage occur, a few extending continuously throughout the study area. The upper, and in places, the lower VSC sequences are commonly stacked in tectonic sheets that were thrusted over the structurally lower Mértola Formation rocks. There are also Late Variscan near-vertical faults in two main families: NW–SE, dextral, and NE–SW, sinistral, both in places with small deposits and occurrences mostly of Cu, but also of Ba(Pb) and Sb(AU) (Matos et al. 2003; Reiser et al. 2011; Oliveira et al. 2004, 2013; Inverno et al. 2015b, see location in Matos and Filipe 2013). Mn–Fe small deposits related to VSC upper sequence lithologies are known at NW Neves-Corvo and Alcoutim (Leca 1976; Leca et al. 1983; Matos and Filipe 2013).

Geophysical methods

2D seismic reflection data

Acquisition

As stated above, several seismic profiles were acquired by CGG in 1991 and 1996 (Carvalho et al. 1996). When interpreted in a GIS environment integrated with drill-hole, geological mapping and other geophysical data, their input suggested that important structural information could be retrieved from the seismic data. Therefore, six 2D seismic profiles, approximately NE–SW oriented, with a total length of 82 km were planned for the area between the Neves-Corvo mine and the Portuguese/Spanish border (Fig. 1). The location of the seismic profiles was chosen to investigate the crust below the flysch cover for the possible extension of the Neves-Corvo volcanic axis to the Alcoutim area (close to the Spanish border), where the VSC outcrops again, and its southern region; along this extension, the VSC rocks were intersected by exploration drill-holes at 400–810 m depth (Billinton exploration project developed in the 1980s). Figure 1 shows a geological map with the location of the six seismic profiles.

Due to the required depth of penetration (4–5 km), either explosives or heavy vibrators are needed to be used as seismic sources. Permits, licenses and the invasive nature of explosives led altogether to the choice of using vibrators. Three synchronized ION AHV-IV vibroseis trucks of 28.5 tonnes each were therefore used as seismic source. A linear

Table 1 Acquisition parameters of the Promine seismic reflection profiles used in this study

Seismic source	Sweep freq. (Hz)	Offset range (m)	Active channels	Channel spacing (m)	Receivers per channel (linear array)	Source move-up (m)	Nominal CMP fold
Three synchronized 28.5-tonne each vibrators	10–90	25–12,000	480	25	6	50	120

Table 2 Major steps of the different processing flows applied to the Promine seismic reflection profiles used in this study

Flow 1	Flow 2	Flow 3	Flow 4
CMP/crooked line geometry	CMP/crooked line geometry	CMP/crooked line geometry	CMP/crooked line geometry
Trace editing + freq. filtering	Trace editing + freq. filtering	Trace editing + freq. filtering	Trace editing + freq. filtering
Muting	Muting	Muting	Muting
Refraction statics	Refraction statics	Refraction statics	Refraction statics
Flat datum conversion	Flat datum conversion	Flat datum conversion	Flat datum conversion
FK filtering	FK filtering	FK filtering	FK filtering
Spiking deconvolution	Spiking deconvolution	Spiking deconvolution	Spiking deconvolution
Velocity analysis	Velocity analysis	Velocity analysis	Velocity analysis
Residual statics	Residual statics	Residual statics	Residual statics
Final datum correction + velocity analysis	**NMO + DMO + stack**	FX decon + CRS geometry	FX decon + CRS geometry
Kirchhoff PSTM	**Dip Explicit FD Time Migration**	PSTM sequence	CMP stack sequence
FX filtering + AGC	**FX filtering + AGC**		

Text in italics indicates PSTM sequence mentioned in flow 3 and text, while text in bold represents CMP stack sequence referred to in flow 4 and text

sweep of 16 s was used with a frequency varying between 10 and 90 Hz to allow recording shallow and deeper reflections. Two or three vibrations per vibration point were carried out.

The data acquisition system used was a Sercel 428 E-Unite Full. SG 10-Hz receivers were used to record the seismic wave field, which was sampled at a 2-ms rate for 6 s. The acquisition parameters are presented in Table 1. The use of a wireless system allowed a superior flexibility in data acquisition. Villages, roads, small rivers could be easily crossed, and the initial design of the profiles could be followed more closely.

Taking into consideration the actual frequency content of the recorded data and the velocities obtained during data processing (see next section), we can expect, using the Rayleigh criterion (Born and Wolf 1980), a maximum vertical resolution of approximately 12 m at shallow depths and of around 150 m at large depths. Horizontal resolution, given by the first Fresnel zone, is approximately 100 m and 1 km for depths of 0.5 km and of 4 km, respectively.

Data processing

Several processing sequences were attempted for each profile: a standard processing sequence, with pre-stack time migration (PSTM) and post-stack migration, and a second processing sequence, with the common-reflection surface (CRS) method (Mann et al. 1999), and followed again by PSTM and post-stack migration.

All processing sequences, listed in Table 2, were similar until the application of residual statics. From this point onwards, the standard and PSTM processing sequences diverged. The CDP gathers were either NMO (normal move-out) and DMO (dip move-out) corrected, stacked and post-stack processed with F-X deconvolution plus AGC applied, and/or prepared for PSTM. In the former case, Steep Dip Explicit Finite Difference Time Migration was applied to the stacked sections, whereas in the latter case, the CDP gathers were prepared for PSTM. Subsequently, a correction to the final datum was applied, a detailed velocity analysis undertaken, and a 2D Kirchhoff time migration algorithm with an aperture of 3–5 km was applied to the gathers. To conclude the processing sequence, FK filters and AGC followed and finally, CDP stack. F-X deconvolution and AGC were applied to the stacks.

The CRS processing sequence was identical to the previous one till the pre-PSTM gathers and before NMO correction. After the application of residual statics to the gathers, the following steps were taken: F-X deconvolution, AGC, 2D CRS ZO search and 2D CRS stack. From this

point onwards, the sequence was different for standard and PSTM sequences. NMO correction and CDP stack (applying statics to final datum) followed by Steep Dip Explicit FD Time Migration for the standard sequence and, for the PSTM flow, corrections to final datum, velocity analysis, PSTM, FK filters and finally stacking. Post-stack processing included F-X deconvolution filtering and AGC (Table 2).

DMO and migration were essential to improve the imaging of steeply dipping features in the data (e.g. Malehmir and Juhlin 2010; Cheraghi et al. 2012). The CRS stacked sections generally resulted in a clear improvement of the signal-to-noise ratio and a better continuity of the seismic reflectors. However, for line 3 (Fig. 2), the CRS stack increased the presence of conflicting dips, probably due to the structural lateral variations in the region and/or an inappropriate velocity function. CRS stacking is particularly sensitive to dip and curvature of the reflectors (Mann et al. 2007), and the local 3D structure might cause additional difficulties in performing an adequate velocity analysis. Figure 2 shows the non-migrated CRS and standard CMP stacks for this line, as well as the post-stack migrated and PSTM stacks.

PSTM sections minimized the effects of conflicting dips (see Fig. 2) in the data that resulted from the 3D nature of the geological structures, but PSTM often introduced probable artefacts (see Fig. 2) in the stacked sections. These artefacts were identified by visual inspection of non-migrated, PSTM and post-stack migrated sections and also taking into account the available geological data. This is also highlighted in Fig. 2 as line 3, but line 6 presents the clearest example. For the final interpretation, it was an advantage to have access to processing sequences and the non-migrated stacks.

Potential-field data

The interpretation of the seismic profiles was complemented with available land gravimetric and aeromagnetic data. In spite of their lower resolution when compared to seismic reflection data, potential-field data can provide valuable information. Magnetic susceptibilities are highly sensitive to lithological variations and can indicate depth variations of VSC units that generally correspond to higher total field magnetic intensities than the surrounding flysch cover, in particular the basic volcanics embedded in the VSC. Density information available from drill-hole data together with gravimetric interpretation can provide information about the presence at depth of denser units such as the PQG, or the possible presence of ore deposits within the VSC. This information is of major importance since seismic data sometimes fail to provide continuous markers between stratigraphic boundaries in hard-rock environments, due to high deformation, overburden compaction and metamorphism.

An unofficial national Bouguer anomaly map based on the National Gravimetric Network (NGN, http://www.igeo.pt/produtos/Geodesia/gravimetria.htm) is available for Portugal mainland. The NGN is constituted by over 6500 points and two absolute stations, one in northern Portugal and the other in southern Portugal, resulting in a minimum density coverage of 1 data point per 25–30 km^2. However, several local gravimetric surveys have been carried out in the IPB by the National Laboratory for Energy and Geology (LNEG) and its predecessors in the last decades. These land surveys that present a much higher data point density than the NGN have been acquired since the 1960s using different equipment and needed to be homogenized before a final Bouguer anomaly map could be completed. Figure 3 shows the Bouguer anomaly map with the location of the seismic lines overlaid. A reference density of 2.65 g/cm^3 was used to produce the Bouguer anomaly map.

In 1991, Geoterrex conducted a magnetic survey over the Portuguese sector of the Iberian Pyrite Belt for the Rio Tinto mining company using a caesium vapour magnetometer at a constant flight altitude of 90 m (Carvalho 1995; Carvalho et al. 2012). The flight lines had a SW–NE orientation and were generally spaced at 500 m, sometimes 250 m, with perpendicular tie lines. The sampling was carried out every 7.5 m and, taking into consideration noise levels, instrument precision, repeatability, etc., a resolution of approximately 0.1 nT was achieved. The survey, which covers the whole study area, was processed by Geoterrex and is used in this work. We have extracted the IGRF from the magnetic total field intensity data and reduced it to the pole. The results are shown in Fig. 4.

The coincidence of geological bodies and man-made structures with gravimetric and magnetic anomalies (see examples indicated by letters in Figs. 3, 4) suggests that at least working at this scale, the reduction to the pole placed the magnetic anomalies at their appropriate locations.

Integrated interpretation and geological modelling

Due to that the seismic lines were a few kilometres apart, a seismic interpretation package was not used to pick the seismic horizons. All the seismic and other geophysical information, as well as geological mapping and drill-hole data, was integrated within a 3D software environment. It was possible to validate the data in a progressive way, which was important to detect inconsistencies.

Figures 5, 6, 7 and 8 display the final interpretation of seismic profiles 1, 2, 4 and 6. The Bouguer anomaly and reduced-to-pole magnetic total field intensity are plotted at the top of the seismic profiles. The stacked sections are

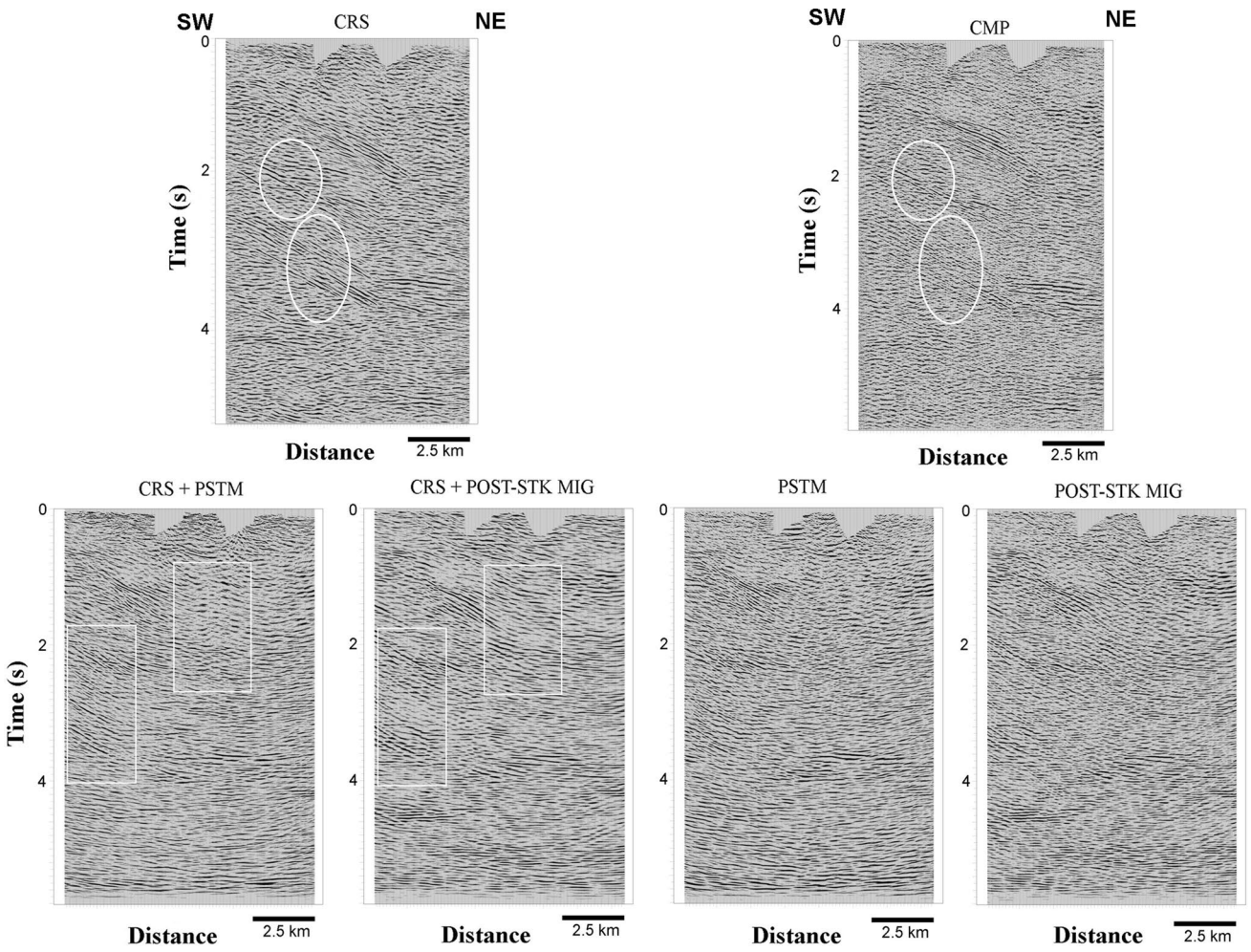

Fig. 2 Stacked sections resulting from the different processing flows applied to seismic reflection profile 3. *Top left* standard CMP stack; *top right* CRS stack; *bottom far left* PSTM CRS stack; *bottom left* CRS stack with post-stack migration applied; *bottom right* PSTM CMP stack; *bottom far right* CMP stack with post-stack migration applied. *Ovals* indicate areas of increased signal-to-noise ratio but also of conflicting dips due to CRS stacking, while *rectangles* show zones of probable artefacts introduced by PSTM and where post-stack migration performs better (see text)

shown with the CRS without migration, and with post-stack time migration, producing much better results than PSTM. All the seismic sections extend to the depths of interest of over 4 km, with the south-eastern lines presenting reflection events down to 10 km. The stacking velocities from the processing were used for depth conversion. These velocities are in agreement with velocity information from drill-holes located in the region of the Neves-Corvo mine (Yavuz et al. 2015) and other drill-holes that reached the Palaeozoic basement in the Lusitanian Basin (GPEP 1986) and also from refraction profiles (Matias 1996).

Three drill-holes, two located 45 m and one about 1 km off line 1 (see Fig. 1) and about 50 m off line 6, intersected a seismic profile. Inspecting for instance profile 1 in detail, drill-hole CT08001, the closest to profile 1, reached a drilled length of 1.89 km and was drilled in 2008 by the AGC/Lundin Mining Company, while drill-hole CT01 had been previously drilled (1.7 km drilled length) by Somincor in 1992. Figure 9 shows the so-called Cotovio geological cross-section based on drill-holes CT08001 and CT01, geological surface data and drill-hole data in the area. To perform the cross-section, CT08001 drill-hole core was re-logged and studied. A careful data interpretation of the CT01 drill-hole was done, based on the 1990s Somincor technical reports. The Cotovio sector geological data were correlated with the information about the geology of the Neves-Corvo mine SE region. Detailed drill-hole geological log data were used in the cross-section and correlated with the seismic profile interpretation. This cross-section has been overlaid with a degree of transparency over the interpreted stacked section of the recently acquired Promine seismic reflection (profile 1) shown in Fig. 5, showing

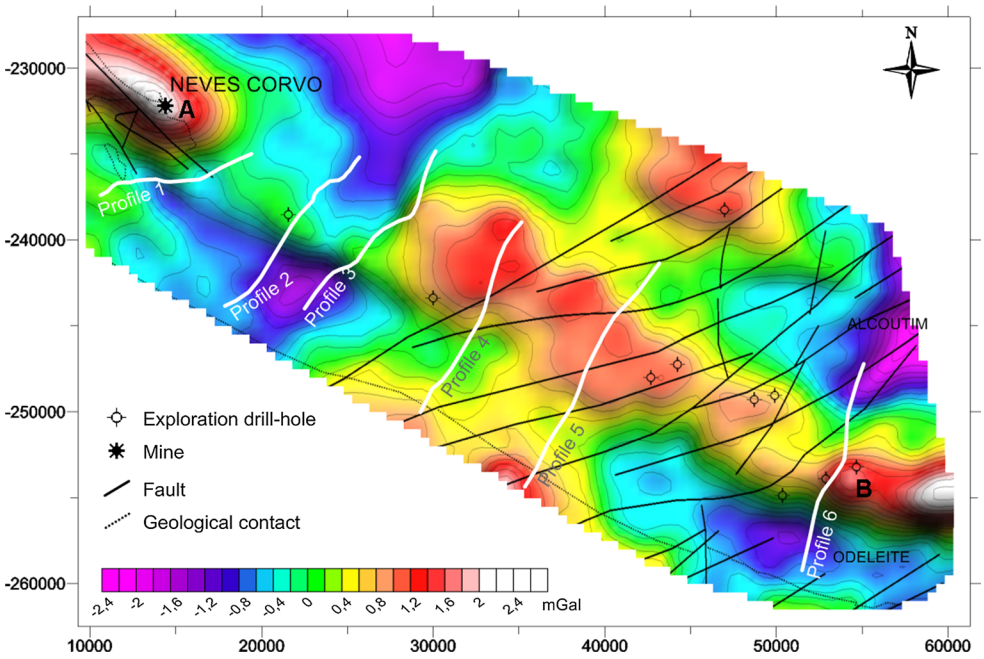

Fig. 3 Bouguer anomaly map available for the study area. The locations of the seismic reflection profiles and available drill-holes are also displayed, together with surface geology contacts and faults (after Oliveira et al. 1992). Coordinates are shown in the Hayford–Gauss system, datum 73, in metres. *Letters* indicate coincidence of gravimetric and magnetic anomalies of the Neves-Corvo mine structure (**a**) and volcanics of the VSC detected by drilling (**b**), suggesting that reduction to the pole correctly placed magnetic anomalies

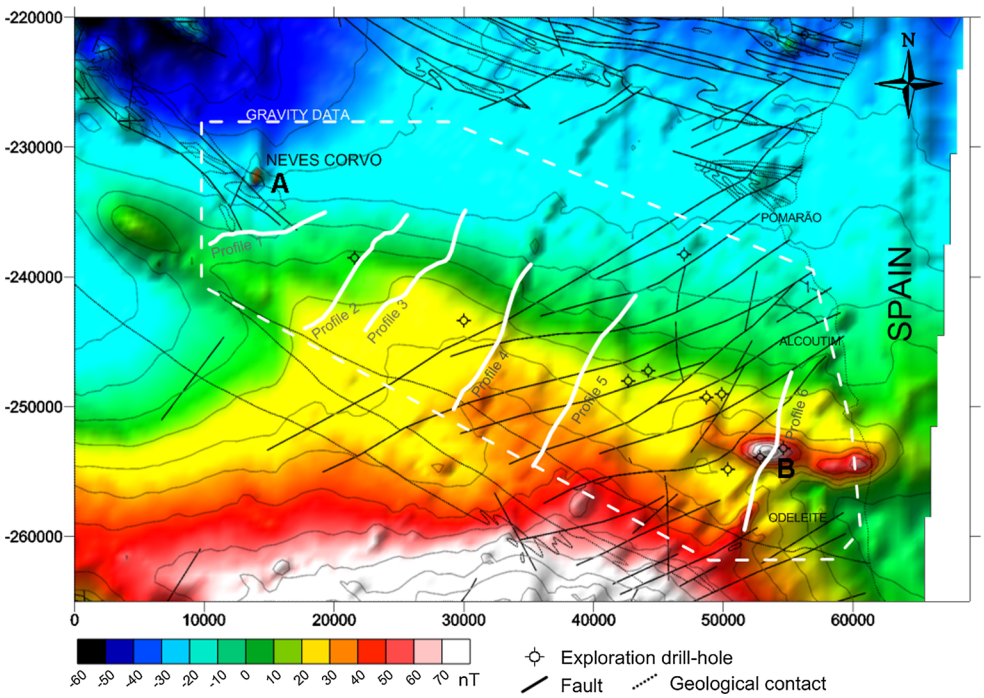

Fig. 4 Total-field, reduced-to-pole aeromagnetic map of the study area, overlaid by the location of the seismic reflection profiles, drill-holes, surface geology contacts and faults (after Oliveira et al. 1992). The area covered by gravimetric data shown in Fig. 3 is indicated. Coordinates are shown in the Hayford–Gauss system, datum 73, in metres. *Letters* indicate coincidence of gravimetric and magnetic anomalies of the Neves-Corvo mine structure (**a**) and volcanics of the VSC detected by drilling (**b**), suggesting that reduction to the pole correctly placed the magnetic anomalies

the seismic/drill-hole tie for profile 1. Once geophysical logs are not available for drill-holes CT08001 and CT01, depth conversion of the seismic horizons was carried out using the seismic data processing velocities. The principal seismic reflectors of profile 1 are also overlaid in Fig. 9. The consistent correlation between seismic data and drill-hole data in the upper part of the profile is represented by the presence of planar reflectors gently dipping to the north-east, corresponding to the boundary between Palaeozoic sedimentary and volcanic rocks.

The Cotovio cross-section, a result of one of the exploration research projects in Iberian Pyrite Belt, provided stratigraphic information down to a depth of 1.6 km in the Cotovio gravity anomaly, located 4 km SE of the Neves-Corvo mine. In both drill-holes (Figs. 5, 9), Baixo Alentejo Flysch and VSC rocks were drilled. In detail, and considering the CT08001 geological log data, the sequence is characterized by shales and greywackes of the Mértola Fm., intersected until 580 m, followed by VSC sedimentary rocks until 1.06 km. Between 1.06 and 1.6 km, felsic

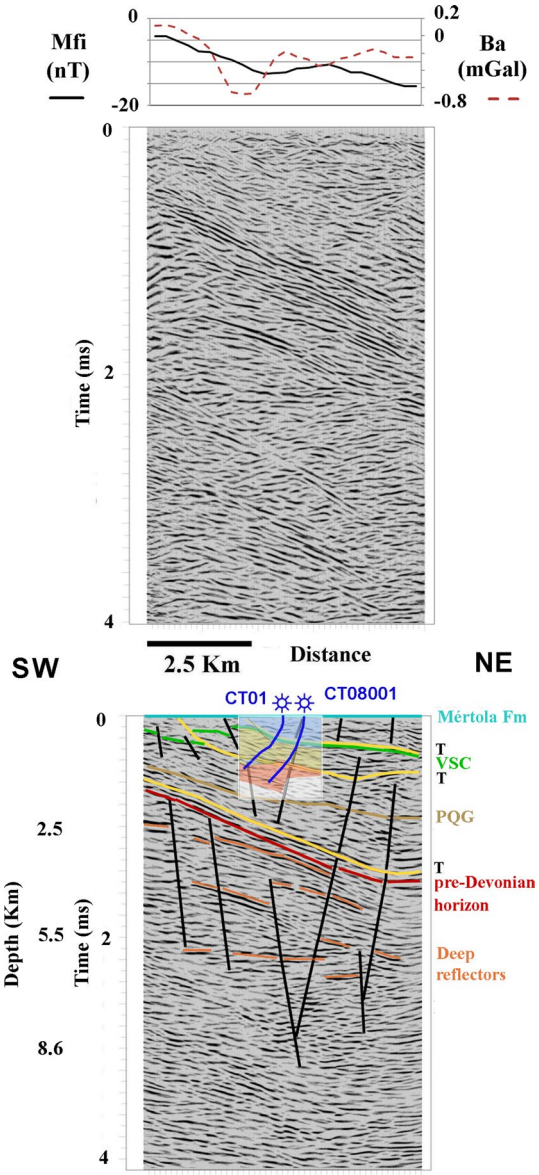

Fig. 5 Gravimetric and magnetic data (**a**) plotted over CRS stack for seismic profile 1 without (**b**) and with post-stack time migration with overlaid stratigraphic and structural interpretation (**c**). The locations of drill-holes CT01 and CT08001 are shown (*blue line*), and a geological cross-section based on these two drill-holes and previously acquired seismic reflection data is overlaid by the interpreted stacked section (see details in Fig. 9). *Mfi* magnetic field intensity (reduced to the pole), *Ba* Bouguer anomaly. *Black lines* faults, *yellow lines/T* thrust planes, *VSC* Volcanic-Sedimentary Complex, *PQG* Phyllite–Quartzite Group, *red line* pre-Devonian horizon, *orange lines* deep crustal reflectors (see text)

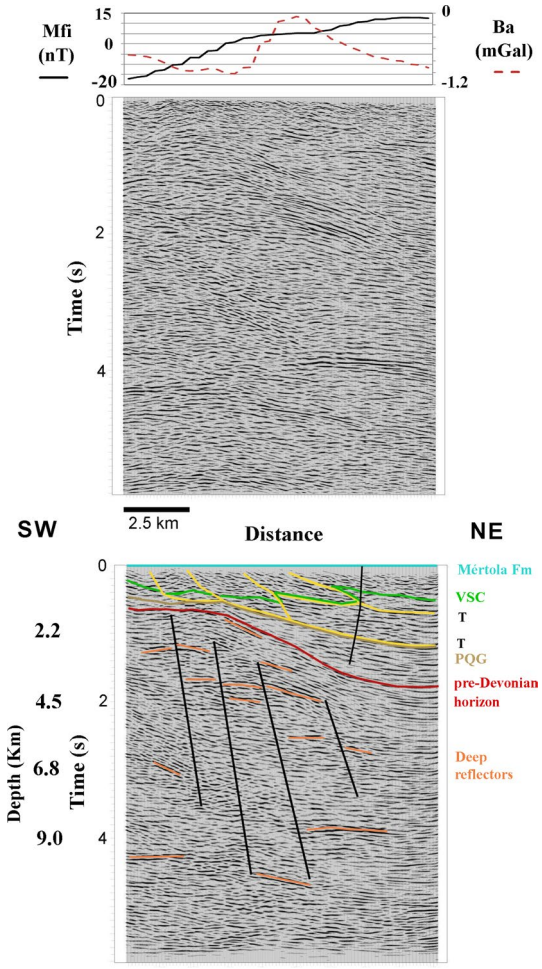

Fig. 6 Gravimetric and magnetic data (**a**) plotted over CRS stack for seismic profile 2 without (**b**) and with post-stack time migration with overlaid stratigraphic and structural interpretation (**c**). *Mfi* magnetic field intensity (reduced-to-pole), *Ba* Bouguer anomaly. *Black lines* faults, *yellow lines/T* thrust planes, *green line/VSC* Volcanic-Sedimentary Complex, *brown line/PQG* Phyllite–Quartzite Group, *red line* pre-Devonian horizon, *orange lines* deep crustal reflectors (see text)

volcanics (rhyolite and rhyodacite) were intersected, representing a large volcanic centre, probably a dome structure. Metric intercalation of VSC sedimentary rocks was observed at 1.52 km, corresponding to a tectonic duplex structure.

The CT01 drill-hole log shows two intersections of shales and greywackes of the Mértola Fm. from 1.02 to 1.08 km and from 1.16 to 1.17 km and reflects the presence of important thrust structures, similar to the Neves-Corvo thrust (Oliveira et al. 2004; Inverno et al. 2015b). These fault plans are related to a strong vergence to SW. None of the drill-holes intersects sulphide mineralization (either massive or semi-massive). Neither do the volcanic rocks show important hydrothermal alteration.

Visible reflector planes (at about 0.2 s) are related to the Mértola Flysch/VSC contact and the VSC sedimentary/volcanic rocks contact (Fig. 5). This surface can be correlated with the top of the Cotovio volcanic structure. The reflectors related to stratigraphy do not show a good lateral continuity along the stacked section of profile 1.

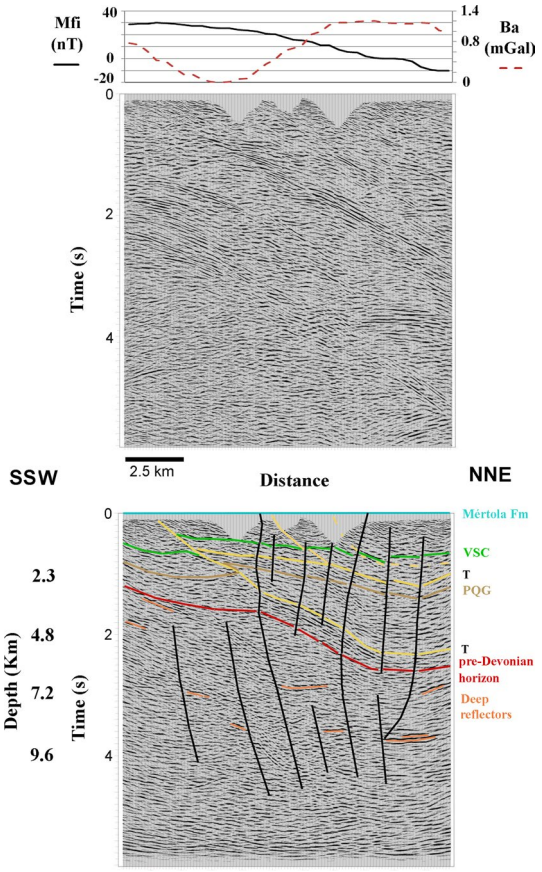

Fig. 7 Gravimetric and magnetic data (**a**) plotted over CRS stack for seismic profile 4 without (**b**) and with PSTM applied, overlaid with stratigraphic and structural interpretation (**c**). *Mfi* magnetic field intensity (reduced-to-pole), *Ba* Bouguer anomaly. *Black lines* faults, *yellow lines/T* thrust planes, *green line/VSC* Volcanic-Sedimentary Complex, *brown line/PQG* Phyllite–Quartzite Group, *red line* pre-Devonian horizon

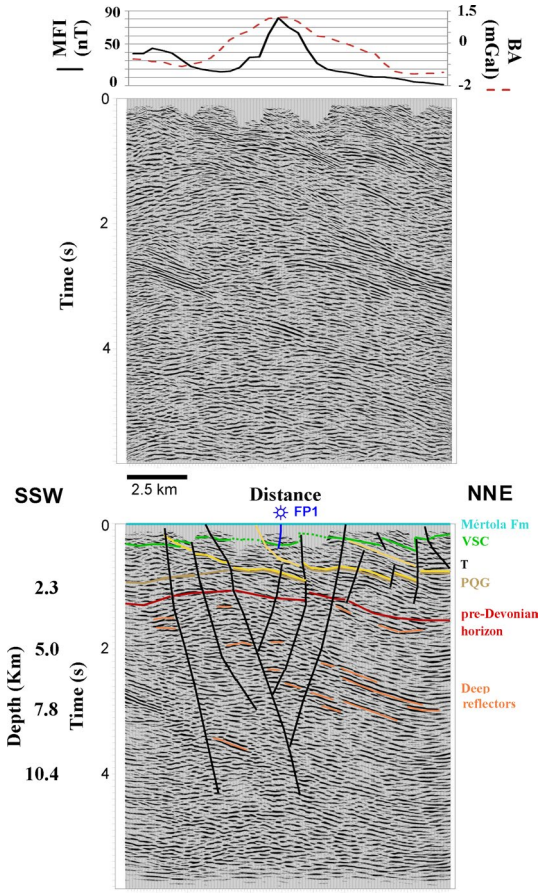

Fig. 8 Gravimetric and magnetic data (**a**) plotted over CRS stack for seismic profile 6 without (**b**) and with post-stack time migration with overlaid stratigraphic and structural interpretation (**c**). *Mfi* magnetic field intensity (reduced-to-pole), *Ba* Bouguer anomaly. *Black lines* faults, *yellow lines/T* thrust planes, *green line/VSC* Volcanic-Sedimentary Complex, *brown line/PQG* Phyllite–Quartzite Group, *red line* pre-Devonian horizon

Recent work carried out in the region of the Neves-Corvo mine (Yavuz et al. 2015), which included the building up of an elastic properties database with measurements on nearly 400 core samples, a modelling study using full-waveform sonic and pseudo-log data to create synthetic seismic data and subsequent tie to 3D seismic reflection data, shows us that the contact between the Mértola Flysch and the VSC is not a prominent reflector compared to intra-flysch reflectors or other stratigraphy-related reflectors. Furthermore, the work of Yavuz et al. (2015) shows us that the strongest amplitude reflectors are related to the presence of massive sulphide deposits (drill-holes PSJ50 and PSK50, in Yavuz et al. 2015). The Mértola Flysch/VSC contact produces at the best (shale/rhyolite contact in drill-hole SZ24A; Yavuz et al. 2015) a much lower reflectivity than massive ore. In our opinion, the flysch/VSC contact reflectivity at drill-hole SZ24A is enhanced by the stratigraphic inversion related to a thrust fault. This reinforces the importance of the structural control in the reflectivity observed in the seismic data (discussed ahead).

Also according to the study of Yavuz et al. (2015), the contact VSC/Phyllite–Quartzite Group (PQG) provided a moderate reflector in drill-hole SZ24A. Deep seismic reflectors at a depth of about 2 km (approximately 0.8 s) in profile 1 are also probably related to the VSC/PQG sedimentary rocks contact. The deeper reflectors below 2 km may correspond to the geological basement rheologic discontinuities. Until the present time, these geological features have not yet been intersected by exploration drill-holes.

Several seismic reflectors related to the low-angle thrust planes were found, in both the former CGG profile and profile 1 acquired in this study (see Figs. 5, 6, 7, 8). These reflectors have a better lateral continuity in the stacked sections compared to stratigraphy-associated reflectors.

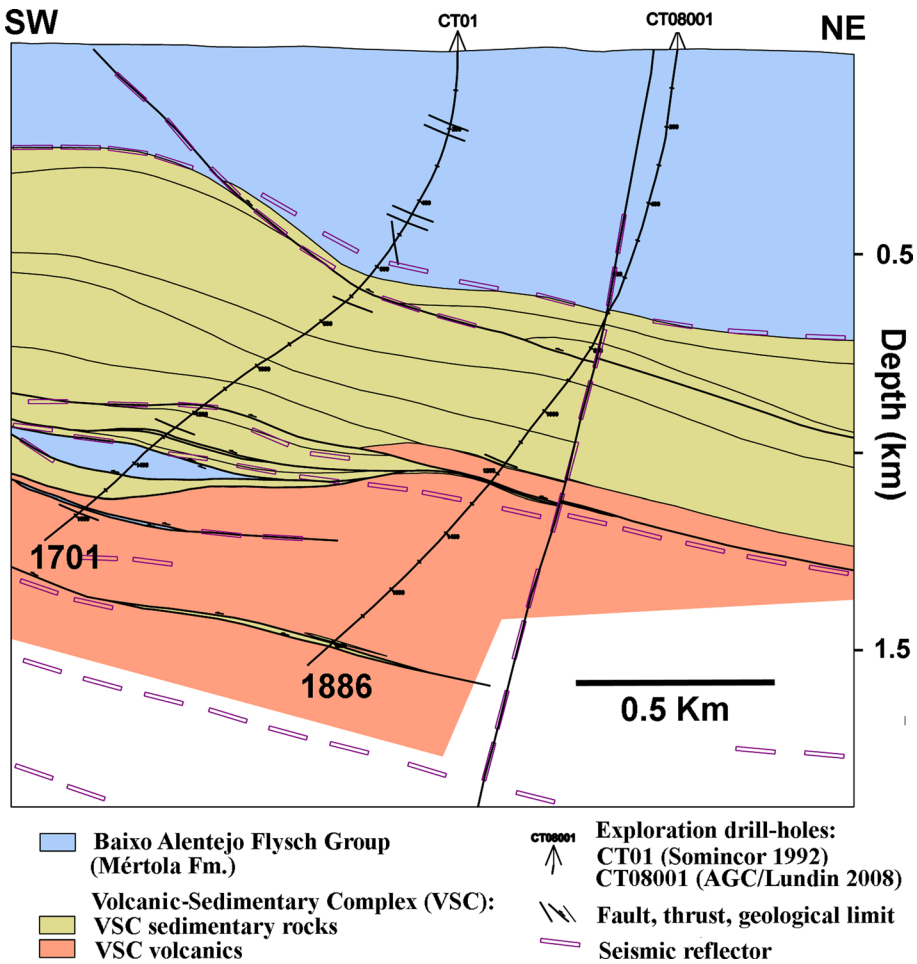

Fig. 9 Cotovio geological cross-section based on the logs of drill-holes CT01 (Somincor, 1992), CT08001 (AGC/Lundin Mining, 2008) and surface geological data. Reflectors observed in the seismic reflection profile 1 acquired in this study are also shown. See location of drill-hole data in Fig. 11. *Numbers* indicate total drilled length (not corrected for drill-hole deviation). Geological formations considered: Mértola Formation (Baixo Alentejo Flysch Group, Upper Visean): shales and greywackes; IPB Volcanic-Sedimentary Complex: sedimentary rocks-Brancanes Fm., shales; Godinho Fm., siliceous shales; Borra-de-Vinho Fm., *purple/green* shales; Grandaços Fm., siliceous shales with nodules; Jaspers and cherts; volcanics-rhyolite and rhyodacite

Other holes located close to the seismic profiles were used to provide a seismic stratigraphy approach to the seismic interpretation. However, drill-hole data in the study area do not provide information on the stratigraphy at depths over 2 km. Therefore, several deep seismo-stratigraphic packages that could be observed in the seismic profiles underneath the PQG remain to be identified, since they were never reached by any drill-holes to date and are not known on the surface. A change of the seismic character (reflectivity pattern and frequency content) was identified in all profiles below a certain depth, often topped by a moderate to strong reflector(s). The seismic horizon that corresponds to pre-Devonian geological units is marked in red in Figs. 5, 6, 7 and 8.

The 3D model building did not include these deep geological units because they are deeper than present-day exploitation capabilities. However, the profiles show the presence of tectonic structures, probable low-angle thrusts, that control the geometry of the Palaeozoic basement. These thrusts also show a tangential deformation dominated by a significant SW vergence. These data are well correlated with the tectonic models defined by the existing exploration drill-hole data, limited to 1–1.5 km depth.

As stated above, potential-field data were also used qualitatively to assist in the interpretation, particularly aeromagnetic data which present the largest coverage of the project area. The Bouguer anomaly map was very useful in defining the orientation of Late Variscan vertical strike-slip faults that offset the Variscan geological faults and horizons, controlling Late Variscan horsts and grabens. The Bouguer anomaly map was also used to confirm the geometry of the deeper and higher-density seismo-geological layers. Together with aeromagnetic data, it provided information about depth variations of the VSC along and across the profiles, also allowing to infer the presence of possible significant massive sulphide deposits.

The major characteristics of the seismic profiles are the presence of several parallel high-angle thrusts, nappes and the presence of several strike-slip faults with minor normal component that cut across the former thrusts. Those strike-slip faults locally host small Late Variscan Cu (and other metals) vein deposits and occurrences (Carvalho 1991; Matos et al. 2003; Reiser et al. 2011; Matos and Filipe 2013), mostly forming a NW–SE Cu lineament anchored in Neves-Corvo mine and in close proximity to Neves-Corvo

extended thrust (see location in Fig. 1). A large NNE–SSW oriented fault, near-parallel and very close to profile 4, probably of Late Variscan age, can be seen on both gravimetric and magnetic data (Figs. 3, 4).

We have also marked several deep strong seismic reflectors within the basement (beneath the pre-Devonian horizon shown in Fig. 5, 6, 7, 8). These deep high-amplitude reflectors in vertical incidence reflection seismic data are usually associated with either fluids or igneous intrusions (e.g. Carbonell et al. 2004; Brown et al. 2012) and increased fracturing (e.g. Schmelzbach et al. 2008a). It is also probable that some of them are out-of-the-plane energy due to a 3D geological environment with intense faulting and strong lateral velocity variations. Those high-amplitude events that cut across other reflectors are likely to have this origin.

Some of the deep reflectors have a similar orientation, structure and amplitude of those observed in a deep seismic reflection profile acquired nearby in Spain, close to the border with Portugal and covering IPB terrains (Schmelzbach et al. 2008a, b). These deep reflectors were interpreted as thrusts and fold belts, major faults and sometimes as mafic intrusions possibly associated with the VSC (Schmelzbach et al. 2008b). Similar reflectivity patterns observed in another deep seismic reflection profile acquired over Palaeozoic terrains of the Central Iberian Zone have also been interpreted as imbricate thrust systems (Ehsan et al. 2014).

The 3D structure of the study area, resulting from the lateral profile-to-profile interpretation, was also constrained using gravimetric and magnetic data. Figure 10 shows a 3D structural model based on the interpretation of the geophysical, drill-hole and geological data. In general, a subsurface 3D model may be obtained by the creation of geological regions within the study area (Almeida et al. 1993; Ferreira et al. 2010; Charifo et al. 2012). In the current research work, the 3D structural models were obtained by the creation of the transition surfaces between the following main groups: flysch (Mértola and Mira Formations), VSC and PQG. In order to improve the 3D model precision, several geological sections were defined along the study area, introducing a regional geological model. The interpretation of the stacked seismic sections was important, because they delineated the known faults to depth from the surface geological maps and drill-holes, and the identification of formation discontinuities.

The modelling was carried out using gOcad (Paradigm 2014), and all the relevant data were represented in the 3D environment. First, an initial model representing the main geological features was constructed, including the extension of the structural framework from Neves-Corvo to the SE (Spanish border). It was important that the behaviour of structures such as other thrusts, nappes and late faults should be demonstrated as well. Thus, based on geological mapping, drill-hole geological data and geophysical data, the fault offsets were inferred. Secondly, another 3D model was defined incorporating the fragmentation of the upper and lower basal surfaces of the formations, with the corresponding fault offsets. The resultant model validation was carried out by overlaying drill-hole data and geological mapping with interpreted seismic stacked sections and other geophysical data (Inverno et al. 2015a).

Figure 11 shows the location of the seismic profiles over a more detailed geological map after Oliveira et al. (1988). This map also shows the location of a NW–SE oriented geological cross-section extracted from the 3D model and therefore based on geological, drill-hole and geophysical data (Fig. 11b). This figure also shows reduced-to-pole total field magnetic intensity and Bouguer anomaly profiles along the cross-section (Fig. 11c).

It is noteworthy that there is an increasing deepening of pre-Devonian basement from seismic profile 1 to profile 4, in particular in the north-eastern part of the profiles (Figs. 10a, 11). In profiles 5 and 6, particularly in the north-eastern side of the profiles, the average depth of the pre-Devonian units rises relative to the depths observed in profiles 1–4. At shallower depths, seismic data show that there is a deepening of the ore-bearing VSC unit to the SE from profiles 1 to 4. Aeromagnetic anomalies related to the IPB Rosário–Neves-Corvo volcanic axis show a loss of amplitude to the SE in this region, which suggests that, taking into account drill-hole, gravimetric and seismic data, there is deepening of the volcanic axis in this area. This deepening is progressive from the Neves-Corvo mine area (see location in Figs. 1 and 11), where the VSC outcrops for a few kilometres, to the SE of it. According to seismic, drill-hole and potential-field data in the region covered by profiles 5 and 6, the top of the VSC is shallower again. Adjacent to the border with Spain, in the Alcoutim region, the VSC does outcrop in a local horst-type structure (Leca 1976).

Discussion

The CRS processing has clearly improved the signal-to-noise ratio of the seismic data, but it also enhanced little side-scattered events and conflicting dips (see Fig. 2). This is due to strong geological lateral changes present in the study area and sensitivity of CRS stacking to velocity analysis (e.g. Mann et al. 2007). PSTM removed conflicting dips, but at the cost of introducing artefacts. DMO and post-stack migration supplied better results possibly because DMO performs better in anisotropic media (Hale 1984; Anderson and Tsvankin 1997) than the 2D Kirchhoff algorithm used in PSTM which usually cannot handle geological complex media (e.g. Yilmaz 2001).

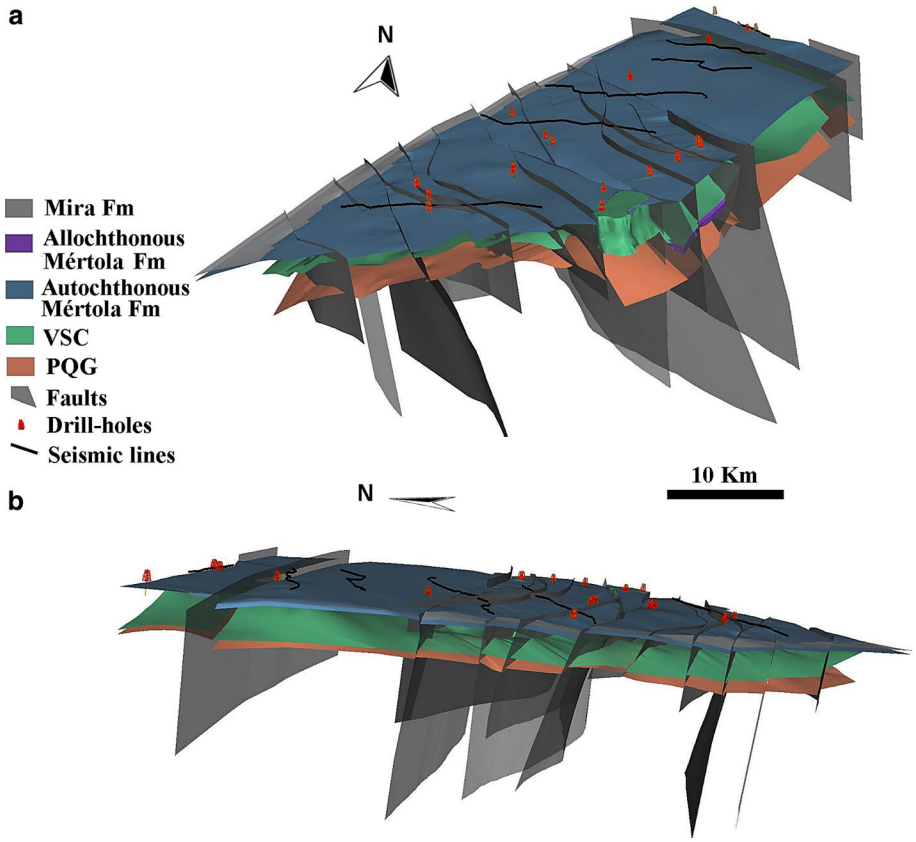

Fig. 10 Two views [**a** view from SE; **b** view from WSW] of the 3D structural stratigraphic model constructed after the integration of drill-hole, geological and geophysical data (seismic reflection, radiometric, gravimetric and magnetic). *VSC* Volcanic-Sedimentary Complex, *PQG* Phyllite–Quartzite Group

As evidenced by several authors, to image steeply dipping structures observed in seismic data, DMO and migration are essential processing steps (e.g. Malehmir and Juhlin 2010; Cheraghi et al. 2012). Schmelzbach et al. (2008b) found good results by applying PSTM, preceded by application of an f-k DMO algorithm to seismic data acquired in the IPB close to the study area, which seems to reinforce the importance of DMO followed by an adequate velocity analysis to image correctly geologically complex media.

DMO and post-stack migration did not completely resolve the problem of conflicting dips. In part, this was caused by the geological complexity of the media and the presence of out-of-the-plane energy. As also pointed by other authors (e.g. Juhlin et al. 2010; Ehsan et al. 2014), the crookedness of some parts of the seismic lines may have also contributed to this fact. However, if we compare profile 1 (Fig. 5) which had a linear geometry with the other seismic lines (Figs. 6, 7, 8), we are led to think that the complexity of the media was the main cause for the remaining conflicting dips after the application of DMO or PSTM.

Anisotropic DMO, advocated for vertically transverse isotropic (VTI) or orthorhombic media (Anderson and Tsvankin 1997; Yilmaz 2001; Tsvankin 2012), was not used in the processing flow due to strong deformation and the steep dips present in the region. These geological aspects, associated with the crooked geometry of the seismic profiles, introduced a strong variation of Thompson parameters along the lines. Therefore, the anisotropy models (e.g. VTI media or the weak anisotropy approximation) under which commercially available anisotropic DMO algorithms are valid are inappropriate for our dataset.

The velocities used to stack the data varied from around 3 km/s at the surface to about 5.5 km/s at 2 s, values that are similar to those used to process other seismic data acquired over the crystalline basement of Iberia (Yavuz et al. 2015; Schmelzbach et al. 2008b; Ehsan et al. 2014; González et al. 1998; Flecha et al. 2006). The high-fold data (120), noise suppression techniques such as the use of 6 receivers per station, the high power and frequency content of the seismic source and the long offsets used to record the data all contributed to the good quality of the stacked sections presented here.

On comparing the magnetic signature of the Neves-Corvo mine area and of the region around profiles 3 and 4 (Fig. 4), there is a clear loss of magnetic field intensity around Neves-Corvo in the NW–SE to WNW–ESE oriented anomalies related to the volcanic axis. This is probably due to the presence of more felsic volcanic rocks compared to basic volcanics. There is a clear positive increase in the amplitude of magnetic anomalies related to this axis in the region of the seismic reflection profile 6, located SW of Alcoutim, near the Spanish border. The

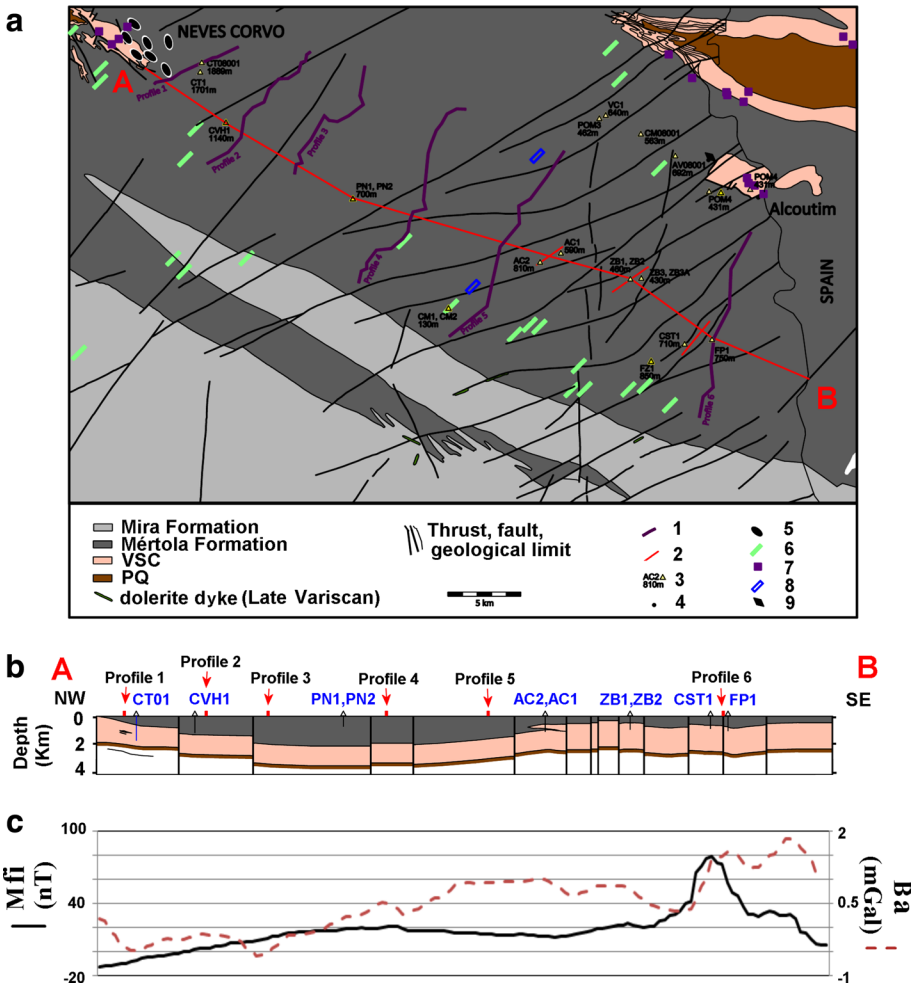

Fig. 11 **a** Geological map after Oliveira et al. (1998) with location of seismic reflection profiles acquired in this study, **b** NW–SE longitudinal geological cross-section (*a*–*b*) along the study area based on drill-hole, geological outcrop and seismic reflection data and **c** respective magnetic field intensity (Mfi) and Bouguer anomaly (Ba) profiles. Surface geology. *1* seismic reflection profile, *2* cross-section, *3* drill-hole and depth of the local geological cross-section, *4* localities, *5* massive sulphide deposits, *6* Cu vein, *7* Mn oxides, *8* Ba–Pb vein, *9* Sb vein

increase in magnetic field intensity related to the volcanic axis can have three main possible causes: (1) a shallowing of the volcanic rocks; (2) an increase in the volume of volcanic rocks; or (3) an increase of basic volcanic rocks relative to felsic volcanic rocks. Shallowing of the VSC is present since it can be found in outcrop near Alcoutim. Here, slates, siltites, jaspers and volcanic sediments can be found (Leca 1976). About 10 km south-west of Alcoutim, VSC units, including felsic and basic volcanic rocks, have been drilled by Billinton in the 1980s at depths between 0.4 and 0.81 km.

The presented seismic data strongly suggest that the ore-bearing IPB VSC extends from the Neves-Corvo mine region at least to the Spanish border near Alcoutim. They show several thrusts and nappes verging to the south-west and the extension of the tectonic setting of the Neves-Corvo mine area along the volcanic axis (hidden) to the Spanish border and possibly further east (Inverno et al. 2015a). At least three major thrusts that reach the surface or come close to it can be tracked from profile to profile (Figs. 5, 6, 7, 8). On the up-thrust blocks of the faults, potential-field and drill-hole data show bodies of felsic and basic volcanic rocks at depths of 400–500 m, which are within present-day exploitation capability.

The regions SE of Neves-Corvo (profiles 1 and 2) and W of Alcoutim–Odeleite (profiles 5 and 6) are the most promising in terms of massive sulphide deposits exploration. In the other seismic profiles, the geological and geophysical data complexity of the study area precludes for the moment any simple conclusion about the possibility that these volcanic bodies bear massive sulphide deposits. In some parts of the region where these volcanic bodies are placed at shallower depth, a similar geophysical signature to that of the Neves-Corvo mine occurs (i.e. intermediate-low magnetic field intensity and high Bouguer anomaly). This is the case for the central part of profile 2 (Fig. 6), the centre of the southern part of profile 6 (Fig. 8) and the central part of profile 5 (Inverno et al. 2015a). Other deeper inclined reflectors observed in the seismic stacked sections may be associated with thrust planes deeply rooted in the upper crust, similarly to the tectonics apparent in the afore-mentioned nearby ALCUDIA (Martínez-Poyatos et al. 2012; Ehsan et al. 2014) and IBERSEIS (Simancas et al. 2003; Schmelzbach et al. 2008b) profiles.

Conclusions

Six 2D seismic reflection profiles were acquired, processed and interpreted to check the possible extension of the Palaeozoic volcanic axis (represented by the Volcanic-Sedimentary Complex) of the Iberian Pyrite Belt beneath the flysch cover to the region SE of the Neves-Corvo mine up to the Spanish border, south of Alcoutim. The geometry of the seismic surveys and the source used were designed to map subsurface features to depths of 4–5 km. The Unite Sercel wireless equipment allowed flexibility and continuous recording across villages and streams, while three synchronized 28-tonne each vibrators provided energy to be recorded down to depths of 10 km.

Several processing sequences were attempted with post-stack and pre-stack time migration, common- and standard common-depth point stacking. Common-reflection surface stacking provided a better signal-to-noise ratio, while pre-stack time migration often introduced artefacts due to the highly complex 3D geological environment, with heavy faulting, thrusting and deformation and the lack of good velocity data. The seismic interpretation, carried out in a 3D environment, was complemented with geological, drill-hole, radiometric and potential-field data. Several SW-verging thrust faults and nappes were identified in the seismic profiles. These structures are cut by multiple Late Variscan strike-slip faults, sometimes with minor normal component, also identified by the seismic data.

The VSC units deepen from the region of the Neves-Corvo mine (where they outcrop) and in profile 1 to profile 4, located further SE. East of profile 4, along profiles 5 and 6, the VSC rises and is located at depths of 400–500 m. Drill-hole data very close to profile 6, located south of Alcoutim and near the Spanish border, show the presence of VSC basic and acid volcanic rocks. The extension of the volcanic axis and of its structural framework from the Neves-Corvo mine to Alcoutim, together with the depth of VSC units in the SE part of the studied area, shows the existence within the IPB of new promising exploration areas. This may lead to the discovery of polymetallic massive sulphide deposits of the Neves-Corvo type.

More detailed geophysical exploration surveys should be carried out in the near future, considering the detailed characterization of geological structures in the volcanic axis(es). The integration of seismic data with other methods (magnetic, gravimetric, drill-holes logging and rock dating) may define consistent geological/geophysical models and their future investigation with deep exploration drill-holes. In this context, the Neves-Corvo geological sequence becomes a reference guide to the Neves-Corvo–Alcoutim IPB region exploration.

Acknowledgments All the facilities in the seismic equipment rental and logistics by Prospectiuni are strongly appreciated by the authors. The authors are grateful to Delfim de Carvalho for all his suggestions and encouragements to write this paper. We are also indebted to Musa Manzi, Christopher Juhlin and anonymous reviewers for their constructive criticism which has significantly improved the manuscript. We are also grateful to LNEG for all support to the logistics of the work, providing equipment, facilities and the personnel involved during the acquisition. Daniel Oliveira, Coordinator of the Department of Mineral Resources and Geophysics of LNEG, is particularly acknowledged. The authors thank all LNEG staff involved in the hard field work. We are also indebted to Lundin Mining and J. M. Castelo-Branco for providing drill-hole and aeromagnetic data used in this work. The authors thank the European Union for financing the Promine project (Nano-particle products from new mineral resources in Europe—228559) under the scope of the FP7 framework, which allowed the acquisition of the seismic data. We are indebted to Rui Vieira from Mohave Oil for the help provided before acquisition of the seismic reflection data.

References

Adam E, Milkereit B, Mareschal M (1998) Seismic reflection and borehole geophysical investigations in the Matagami mining camp. Can J Earth Sci 35:686–695. doi:10.1139/e98-022

Ahmadi O, Juhlin C, Malehmir A, Munck M (2013) High-resolution 2D seismic imaging and forward modeling of a polymetallic sulfide deposit at Garpenberg, central Sweden. Geophysics 78(6):B339–B350

Almeida J, Soares A, Reynaud R (1993) Modelling the shape of several marble types in a quarry. In: Elbrond J (ed) Proceedings of the XXIV international symposium APCOM, Montreal, vol 3, pp 452–459

Anderson JE, Tsvankin I (1997) Dip-moveout processing by Fourier transform in anisotropic media. Geophysics 62:1260–1269

Ayarza P, Juhlin C, Brown D, Beckholmen M, Kimbell G, Pechning R, Pevzner L, Pevzner R, Ayala C, Bliznetsov M, Glushkov A, Rybalka A (2000) Integrated geological and geophysical studies in the SG4 borehole area, Tagil Volcanic Arc, Middle Urals: location of seismic reflectors and source of the reflectivity. J Geophys Res 105:21333–21352. doi:10.1029/2000JB900137

Boogaard MV (1967) Geology of Pomarão region (Southern Portugal). PhD Thesis. Graffisch Centrum Deltro. Rotterdam

Born M, Wolf E (1980) Principles of optics, 6th edn. Pergamon, Oxford

Brown D, Zhang X, Palomeras I, Simancas F, Carbonell R, Juhlin C, Salisbury M (2012) Petrophysical analysis of a mid-crustal reflector in the IBERSEIS profile, SW Spain. Tectonophysics 550:35–46

Calvert AJ, Li Y (1999) Seismic reflection imaging over a massive sulfide deposit at the Matagami mining camp, Quebec. Geophysics 64:24–32. doi:10.1190/1.1444521

Carbonell R, Simancas F, Juhlin C, Pous J, Pérez-Estaún A, González-Lodeiro F, Muñoz G, Heise W, Ayarza P (2004) Geophysical evidence of a mantle derived intrusion in SW Iberia. Geophys Res Lett 31:L11601. doi:10.1029/2004GL019684

Carvalho D (1991) A case history of the Neves Corvo MassiveSulphide deposit and implications for future discoveries, Economic Geology Monograph no 8: historical perspectives of genetic concepts and case histories of famous discoveries, pp 314–334

Carvalho J (1995) Study of the South Portuguese Zone and Adjacent Atlantic margin using geophysical data. M.Sc., Dissertation (in Portuguese), University of Lisbon, Portugal

Carvalho D, Conde L, Enrile JH, Oliveira V, Schermerhorn LJGS (1976) Livro-guia das excursões geológicas na Faixa Piritosa Ibérica, na III Reunião do Sudoeste no Maciço Hespérico da Península Ibérica. Comunicações Serviços Geológicos Portugal 60:271–315 **(in Portuguese)**

Carvalho P, Pacheco N, Beliz A, Ferreira A (1996) Últimos desenvolvimentos em prospeção realizados pela Somincor. Bol. Geologico y Minero ITGE, vol 107 (5–6), Madrid, 39–54

Carvalho D, Barriga FJAS, Munhá J (1999) Bimodal siliciclastic systems: the case of the Iberian Pyrite Belt. In: Barrie CT, Hannington MD (eds) Volcanic-associated massive sulfide deposits: processes and examples in modern and ancient settings, reviews in economic geology 8, pp 375–408, Society of Economic Geologists

Carvalho J, Sousa P, Matos J, Pinto C (2011) Ore prospecting in the Iberian Pyrite Belt using seismic and potential-field data. J Geophys Eng 8(2):142–153

Carvalho J, Matias H, Rabeh T, Menezes P, Barbosa V, Dias R, Carrilho F (2012) Connecting onshore structures in the algarve with the southern Portuguese continental margin: the Carcavai Fault Zone. Tectonophysics 570–571:151–162. doi:10.1016/j.tecto.2012.08.011

Charifo G, Almeida JA, Ferreira A (2012) Managing borehole samples of unequal lengths to construct a high-resolution mining model of mineral grades zoned by geological units. J Geochem Explor 132:209–223

Cheraghi S, Malehmir A, Bellefleur G (2011) 2-D seismic reflection imaging in the Brunswick no. 6 massive sulphide and iron deposits, Bathurst Mining Camp, Canada: implications for crustal architecture and mineral potential. Tectonophysics 506:55–72. doi:10.1016/j.tecto.2011.04.011

Cheraghi S, Malehmir A, Bellefleur G (2012) 3D imaging challenges in steeply dipping mining environment: new lights on acquisition geometry and processing from the Brunswick no. 6 seismic data, Canada. Geophysics 77(5):WC109–WC122

Cordsen A, Galbraith M, Peirce J, Hardage BA (2000) Planning 3-D land seismic surveys, geophysical developments no. 9, Society of Exploration Geophysicists, Tulsa

Eaton DW (2003) Hardrock seismic exploration. Geophysical Development Series No 10, SEG, Tulsa (USA)

Ehsan AE, Carbonell R, Ayarza P, Martí D, Pérez-Estaún A, Martínez-Poyatos DJ, Simancas JF, Azor A, Mansilla L (2014) Crustal deformation styles along the reprocessed deep seismic reflection transect of the Central Iberian Zone (Iberian Peninsula). Tectonophysics 621:159–174

Ferreira A, Charifo G, Almeida J (2010) 3D geologic modeling. The example of the Farim-Saliquinhé phosphates mineralization, Geophysical Research Abstracts, vol 12, EGU2010-10927, EGU general assembly conference abstracts, Viena, Austria, 10927 p

Flecha I, Carbonell R, Zeyen H, Martí D, Palomeras I, Simancas F, Pérez-Estaún A (2006) Imaging granitic plutons along the IBERSEIS profile. Tectonophysics 420:37–47

González A, Cordoba D, Vegas R, Matias LM (1998) Seismic crustal structure in the southwest of the Iberian Peninsula and the Gulf of Cadiz. Tectonophysics 296:317–331. doi:10.1016/S0040-1951(98)00151-6

GPEP (Gabinete para a Pesquisa e Exploração de Petróleos) (1986) Petroleum Potential of Portugal. GPEP, Lisboa

Hale D (1984) Dip-moveout by Fourier transform. Geophysics 49:741–757

Heinonen S, Heikkinen PJ, Kousa J, Kukkonen I, Snyder T, David B (2013) Enhancing hardrock seismic images: reprocessing of high resolution seismic reflection data from Vihanti, Finland. J Appl Geophys 93:1–11. doi:10.1016/j.jappgeo.2013.03.004

Hubral P (ed) (1999) Macro model independent seismic reflection imaging. Journal of Applied Geophysics 42 (3,4)-Special issue on Karlsruhe Workshop on macro model independent seismic reflection imaging. Elsevier, Amsterdam

Inverno C, Rosa C, Matos J, Carvalho J, Castello-Branco JM, Batista MJ, Granado I, Oliveira JT, Araújo V, Pereira Z, Represas P, Solá AR, Sousa P (2015a) Modelling of the Neves Corvo area. In: Weihed P (ed) 3D, 4D and predictive modelling of major mineral belts in Europe, chapter 11. Springer, Berlin, pp 231–261

Inverno C, Diez-Montes A, Rosa C, García-Crespo J, Matos J, García-Lobón JL, Carvalho J, Bellido F, Castello-Branco JM, Ayala C, Batista MJ, Rubio F, Granado I, Tornos F, Oliveira JT, Rey C, Araújo V, Sánchez-García T, Pereira Z, Represas P, Solá AR, Sousa P (2015b) Introduction and geological setting of the Iberian Pyrite Belt. In: Weihed P (ed) 3D, 4D and predictive modelling of major mineral belts in Europe, Chapter 9. Springer, Berlin, pp 191–208

Juhlin C, Stephens M (2006) Gently dipping fracture zones in Paleoproterozoic metagranite, Sweden: evidence from reflection seismic and cored borehole data, and implications for the disposal of nuclear waste. J Geophys Res 111:B09302. doi:10.1029/2005JB003887

Juhlin C, Elming SÅ, Mellqvist C, Öhlander B, Weihed P, Wikström A (2002) Crustal reflectivity near the Archaean–Proterozoic boundary in northern Sweden and implications for the tectonic evolution of the area. Geophys J Int 150:180–197. doi:10.1046/j.1365-246X.2002.01706.x

Juhlin C, Dehghannejad M, Lund B, Malehmir A, Pratt G (2010) Reflection seismic imaging of the end-glacial Pärvie Fault system, northern Sweden. J Appl Geophys 70:307–316. doi:10.1016/j.jappgeo.2009.06.004

Kim JS, Moon WM, Lodha G, Serzu M, Soonavvala N (1994) Imaging of reflection seismic energy for mapping shallow fracture zones in crystalline rocks. Geophysics 59:753–765

Leca X (1976) Le volcano-sédimentaire de la région d´Alcoutim (Baixo-Alentejo-Portugal). Comunicações dos Serviços Geológicos de Portugal, T. LX: 139–149

Leca X, Ribeiro A, Oliveira JT, Silva JB, Albouy L, Carvalho P, Merino H (1983) Cadre géologique dés minéralisations de Neves Corvo (Baixo-Alentejo, Portugal)—Lithostratigraphie, paléogéographie et tectonique. Éditions du BRGM, Orléans, France, Mémoire du BRGM nr. 121-1983

Malehmir A, Juhlin C (2010) An investigation of the effects of the choice of stacking velocities on residual statics for hardrock reflection seismic processing. J Appl Geophys 72:28–38. doi:10.1016/j.jappgeo.2010.06.008

Malehmir A, Dahlin P, Lundberg E, Juhlin C, Sjöström H, Högdahl K (2011) Reflection seismic investigations in the Dannemora area, central Sweden: insights into the geometry of poly-phase deformation zones and magnetite-skarn deposits. J Geophys Res 116:B11307. doi:10.1029/2011JB008643

Malehmir A, Durrheim R, Bellefleur G, Urosevic M, Juhlin C, White D, Milkereit B, Campbell G (2012a) Seismic methods in mineral exploration and mine planning: a general overview of past and present case histories and a look into the future. Geophysics 77:WC173–WC190

Malehmir A, Juhlin C, Wijns C, Urosevic M, Valasti P, Koivisto E (2012b) 3D reflection seismic imaging for open-pit mine planning and deep exploration in the Kevitsa Ni–Cu–PGE deposit, northern Finland. Geophysics 77:WC95–WC108

Mann J, Hubral P, Hocht G, Jaeger R, Mueller T (1999) Applications of the common-reflection-surface stack. In: 69th annual international meeting of the society of exploration geophysicists, pp 1829–1832

Mann J, Schleicher J, Hertweck T (2007) CRS stacking—a simplified explanation, EAGE 69th annual conference and exhibition extended abstracts, London, B044

Manzi MSD, Gibson MAS, Hein KAA, King N, Durrheim RJ (2012) Application of 3D seismic techniques to evaluate ore resources in the West Wits Line goldfield and portions of the West Rand goldfield, South Africa. Geophysics 77:WC163–WC171. doi:10.1190/GEO2012-0133.1

Manzi MSD, Hein KAA, King N, Durrheim RJ (2013) Neoarchaean tectonic history of the Witwatersrand basin and Ventersdorp Supergroup: new constraints from high resolution 3D seismic reflection data. Tectonophysics 590:94–105. doi:10.1016/j.tecto.2013.01.014

Martínez-Poyatos D, Carbonell R, Palomeras I, Simancas JF, Ayarza P, Martí D, Azor A, Jabaloy A, González Cuadra P, Tejero R, Martín Parra LM, Matas J, González Lodeiro F, Pérez-Estaún P, García Lobón JL, Mansilla L (2012) Imaging the crustal structure of the Central Iberian Zone (Variscan Belt): the ALCUDIA deep seismic reflection transect. Tectonics 31:TC3017. doi:10.1029/2011TC002995

Matias L (1996) Experimental seismology in crustal structural modeling in Portugal mainland. Ph.D. Dissertation (in Portuguese), University of Lisbon, Portugal

Matos JX, Martins L, Rosa C (2003) Parque Mineiro da Cova dos Mouros—IGM contribute for the sustainable development of the mining park. IGME, Pub. Museo Geom., no 2, pp 487–494

Matos JX, Filipe A, coord. (2013) Carta de Ocorrências Mineiras do Alentejo e Algarve à escala 1:400 000, digital version. LNEG/ATLANTERRA (Eds), Lisboa. ISBN: 978-989-675-029-9, Coauthors: Oliveira D, Inverno C, Rosa C, Batista MJ, Pereira Z, Salgueiro R, Cunha T, Barreira F. http://www.lneg.pt/download/7904/

Matos JX, Pereira Z, Rosa C, Oliveira JT (2014) High resolution stratigraphy of the Phyllite–Quartzite Group in the northwest region of the Iberian Pyrite Belt, Portugal. Comunicações do LNEG, 7 pp. Actas do Congresso Nacional de Geologia, Porto, Portugal

Matte P (1986) Tectonics and plate tectonics model for the Variscan belt of Europe. Tectonophysics 126:329–374

Menke W (2012) Geophysical data analysis: discrete inverse theory. Academic Press, Amsterdam

Oliveira JT (1983) The marine Carboniferous of South Portugal: a stratigraphic and sedimentologic approach. In: Sousa MJL, Oliveira JT (eds) The carboniferous of Portugal, Memoria Serviços Geológicos Portugal 29, Lisbon, pp 3–37

Oliveira JT coord. (1988) Geological map of Portugal scale 1: 200,000 Sheet No 7, coord. Oliveira JT, Serviços Geológicos de Portugal, Lisboa

Oliveira T et al., coord. (1992) Geological Map of Portugal. scale 1: 500,000, Serviços Geológicos de Portugal, Lisboa

Oliveira JT, Carvalho P, Pereira Z, Pacheco N, Korn D (2004) Stratigraphy of the Tectonically imbricated lithological succession of the Neves-Corvo mine region, Iberian Pyrite belt. Implications for the regional basin dynamics. Miner Deposita 34:422–436

Oliveira JT, Rosa CJP, Rosa DRN, Pereira Z, Matos JX, Inverno CMC, Andersen T (2013) Geology of the Neves-Corvo antiform, Iberian Pyrite Belt, Portugal: new insights from physical volcanology, palynostratigraphy and isotope geochronology studies. Miner Deposita 48:749–766

Paradigm (2014) SKUA-GOCAD™ - Paradigm^{R} 14.1. Release Notes. Paradigm, USA

Pereira Z, Matos JX, Fernandes P, Oliveira JT (2008) Palynostratigraphy and systematic palynology of the Devonian and Carboniferous successions of the South Portuguese Zone, Portugal. Memória 34, INETI, Lisboa

Radzevicius SJ, Pavlis GL (1999) High-frequency reflections in granite? Delineation of the weathering front in granodiorite at Piñon Flat, California. Geophysics 64:1828–1835

Reiser FKM, Rosa DRN, Pinto AM, Carvalho JRS, Matos JX, Guimarães F, Alves LC, De Oliveira DPS (2011) Mineralogy and geochemistry of tin- and germanium bearing copper ore from the Barrigão remobilised vein deposit, Iberian Pyrite Belt, Portugal. Int Geol Rev 53:1212–1238

Relvas JMRS, Barriga FJAS, Ferreira A, Noiva PC, Pacheco N, Barriga G (2006) Hydrothermal alteration and mineralization in the Neves-Corvo volcanic-hosted massive sulfide deposit, Portugal: I. Geology, mineralogy, and geochemistry. Econ Geol 101–4:753–790

Sáez R, Pascual E, Toscano PM, Almodóvar GR (1999) The Iberian type of volcanosedimentary massive sulfide deposits. Miner Deposita 34:549–570

Schermerhorn LJG (1971) An outline stratigraphy of the Iberian Pyrite Belt. Boletim Geológico Mineiro España 82(3–4):239–268

Schmelzbach C, Horstmeyer H, Juhlin C (2007) Shallow 3D seismic reflection imaging of fracture zones in crystalline rock. Geophysics 72:B149–B160. doi:10.1190/1.2787336

Schmelzbach C, Zelt CA, Juhlin C, Carbonell R (2008a) P- and S(V)-velocity structure of the South Portuguese Zone fold-and-thrust belt, SW Iberia, from traveltime tomography. Geophys J Int 175(2):689–712

Schmelzbach C, Simancas JF, Juhlin C, Carbonell R (2008b) Seismic reflection imaging over the South Portuguese Zone fold-and-thrust belt, SW Iberia. J Geophys Res 113:B08301. doi:10.1029/2007JB005341

Simancas JF, Carbonell R, González Lodeiro F, Pérez-Estaún A, Juhlin C, Kashubin A, Azor A, Martínez-Poyatos D, Almodóvar GR, Pascual E, Sáez R, Expósito I (2003) The crustal structure of the transpressional Variscan orogen of SW Iberia: the IBERSEIS deep seismic reflection profile. Tectonics 22:1062. doi:10.1029/2002TC001479

Tsvankin I (2012) Seismic Signatures and analysis of reflection data in Anisotropic Media, Geophysical References Series No. 19, Society of Exploration Geophysicists, Third Edition, Tulsa, USA

Urocsevic M, Ganesh B, Marcos G (2012) Targeting nickel sulphide deposits from 3D seismic reflection data at Kambalda. Australia. Geophysics 77(5):WC123–WC132

Vermeer GJO (2002) 3-D seismic survey design. Society of Exploration Geophysics, Tulsa

Yavuz S, Kinkela J, Dzunic A, Penney M, Neto R, Araújo V, Ziramov S, Pevzner R, Urosevic M (2015) Physical property analysis and preserved relative amplitude processed seismic imaging of volcanogenic massive sulfides—a case study from Neves-Corvo. Port Geophys Prospect 63(4):798–812. doi:10.1111/1365-2478.12269

Yilmaz O (2001) Seismic data analysis: processing, inversion, and interpretation of seismic data, vol 1. Society of Exploration Geophysicists, Tulsa